Copyright © 1996 Elsevier Science Ltd
Paper No. 404. (quote when citing this article)
Eleventh World Conference on Earthquake Engineering
ISBN: 0 08 042822 3

POST-YIELD BEHAVIORS OF MULTI-STORY REINFORCED CONCRETE SHEAR WALLS SUBJECTED TO BILATERAL DEFORMATIONS UNDER AXIAL LOADING

IMANISHI TATSUYA

Technical Research Institute of Matsumura-Gumi Corporation
5-2-2, kanokodai-minami-machi, kita-ku, Kobe, 651-15, Japan

ABSTRACT

This paper reports the experimental and analytical results and their discussion of isolated multi-story reinforced concrete shear walls subjected to bi-lateral deformations under axial loading. The object of this study is to investigate the deformation capacity of shear walls under bilateral earthquake loads. Five shear wall specimens were constructed using 60 MPa grade concrete and 800 MPa grade reinforcement bar. All of the specimens were designed to yield firstly in flexure. Variables of the testing program were; the lateral deformation path, the level of axial stress acting on the wall, confinement of column and wall. Finite filament analysis at the base of the specimen which corresponds to the critical section was carried out to discuss the experimental results.

The deformation capacity of the specimens subjected to bi-lateral deformations were smaller than that of the specimen subjected to uni-lateral deformation. The axial compressive strain in the compression-side boundary column developed during out-of-plane loading as well as in-plane loading. This strain development caused poor deformation capacity of shear walls subjected to bilateral deformations. The confinement of boundary column and wall panel by subtie effectively prevented the development of axial compressive strain and enhanced the deformation capacity of shear wall.

KEYWORDS

Reinforced concrete; shear wall; bi-lateral deformations; ductility; finite filament analysis.

INTRODUCTION

Reinforced concrete shear walls are frequently used in buildings to provide lateral strength and stiffness for wind and earthquake forces. Because of the multi-direction nature of ground motions, structural walls are subjected to vertical load and in-plane and out-of-plane loads simultaneously. However the effect of the inelastic interaction of bilateral deformations is not generally considered in the present structural design. And there is few reference on reinforced concrete shear walls subjected to bi-lateral deformations under axial loading.

However, bi-lateral loadings greatly affects on their deformation capacity as well as load carrying capacity. This effect should be considered particularly in the seismic design of ductile frames. This paper reports the experimental and analytical results and their discussion of isolated multi-story reinforced concrete shear walls subjected to bi-lateral deformations under axial loading, focusing on deformation capacity and load carrying capacity.

TEST PROGRAM

The test program was a partial parametric investigation of wall specimens representing a lower part of multi-story shear walls.

Test Specimens

Table 1 summarizes the properties of test specimens. All specimens have the same horizontal sectional dimensions (with boundary columns of 20cm×20cm, a wall panel 8cm×130cm) and the same height of the wall (200cm). Variable details, as implied in the names of the specimens, M35X through MW35H, in which M or P, indicates the boundary columns with or without subties, respectively, and MW does additional subtie in the wall panel ; 30 and 35 indicate the levels of axial stress acting on the wall; X means uni-lateral deformation path, and H does H-shaped bi-lateral deformations path, respectively.

The test specimens MW35H and M35H are shown in Fig. 1. All of the specimens were designed to yield firstly in flexure. Five flexural type shear wall specimens were the 1/3-scale models of the real structure. All specimens were constructed using Grade 60 MPa concrete and Grade 800 MPa reinforcement bar. The representative compressive stress-strain curves of the compression test of core column element with same details and plain concrete are shown in Fig. 2. The stress-strain curves of reinforcement bars are shown in Fig. 3.

Table 1. Summary of properties of test specimen.

<table>
<tr><th rowspan="2">specimen</th><th colspan="4">boundary column</th><th colspan="3">wall web</th><th>axial load level</th><th rowspan="2">axial load
N
(tonf)</th><th rowspan="2">loading path</th></tr>
<tr><th>width × depth (mm)</th><th>main bar (pg %)</th><th>spiral hoop (pw %)</th><th>sub tie (pw %)</th><th>panel height hw (mm)</th><th>panel thickness × panel length (mm)</th><th>wall web bar (Ps %)</th><th>$\frac{N}{2A\sigma_B}$</th></tr>
<tr><td>M35X</td><td rowspan="5">200
×
200</td><td rowspan="5">12-D10
(2.14)</td><td rowspan="5">D6
@60
(0.53)</td><td rowspan="4">D6
@60
(0.53)</td><td rowspan="5">2000</td><td rowspan="5">80
×
1300</td><td rowspan="5">2-D6
@100
(0.8)</td><td>0.35</td><td>180</td><td>uni-deformation</td></tr>
<tr><td>M30H</td><td>0.3</td><td>150</td><td rowspan="4">H -shape</td></tr>
<tr><td>M35H</td><td rowspan="3">0.35</td><td>196</td></tr>
<tr><td>MW35H</td><td>170</td></tr>
<tr><td>P35H</td><td>-----</td><td>190</td></tr>
</table>

Note;
M or P indicates the boundary columns with or without subties, respectively and MW does additional subtie in the wall panel;
30 and 35 indicate the levels of axial stress acting on the wall;
X means uni-lateral deformation path,and H does H-shaped bi-lateral deformations path .

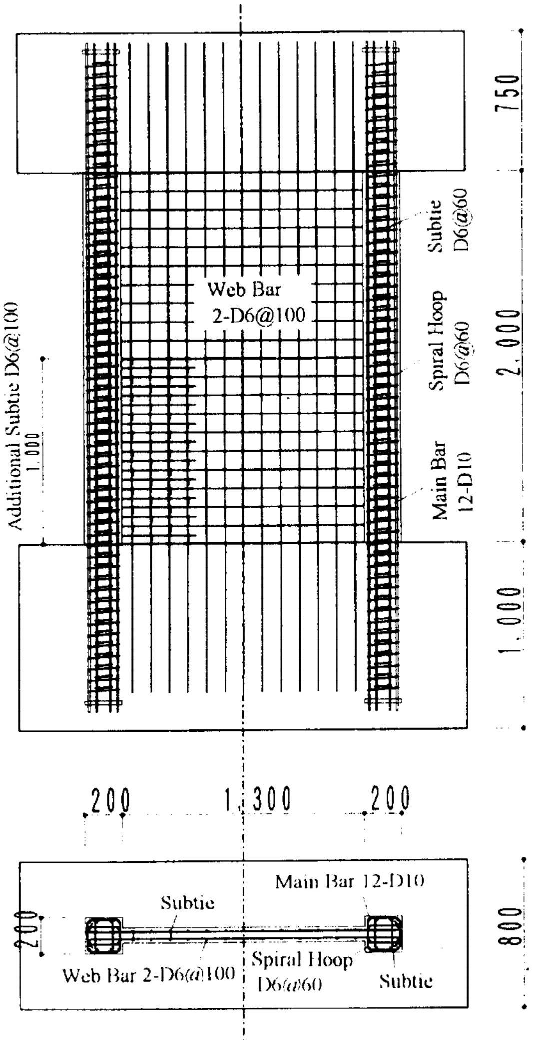

MWtype Mtype

Fig. 1. Test specimen

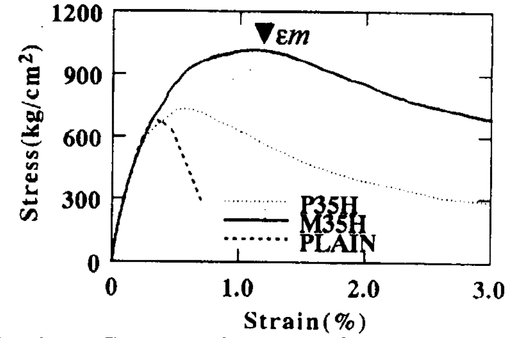

Fig. 2. Compression test of column element

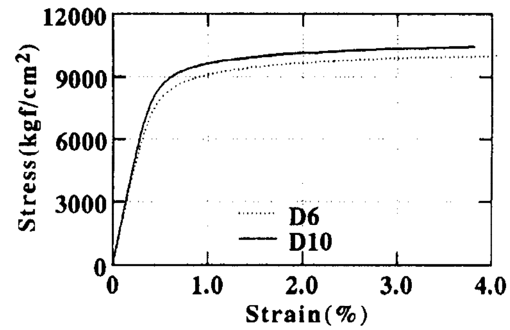

Fig. 3. Tension test of reinforcement bar

Test Procedures

Test setup of loading system is show in Fig. 4. Each specimen was subjected to lateral and vertical loads simultaneously through the top block. Four vertical actuators were used to control the axial load and rotational angle at the top of the specimen. Three horizontal actuators were used to control the two lateral displacements. In-plan loading was controlled that the shear span to depth ratio should be 2.0. And out-of-plan moment diagram was anti-symmetric with shear span to depth ratio of 5.0. In-Plane lateral load was applied by the parallel actuator, which were controlled to prevent torsion deflection. Four vertical actuators were controlled, the following condition should be capability:

$$\sum_{i=1}^{4}(N_{JBi}) = \text{Constant} \quad (1)$$

$$N_{JB3} = N_{JB4} \quad (2)$$

$$N_{JB3} + A_{JB4} = A_{JB1} + A_{JB2} \quad (3)$$

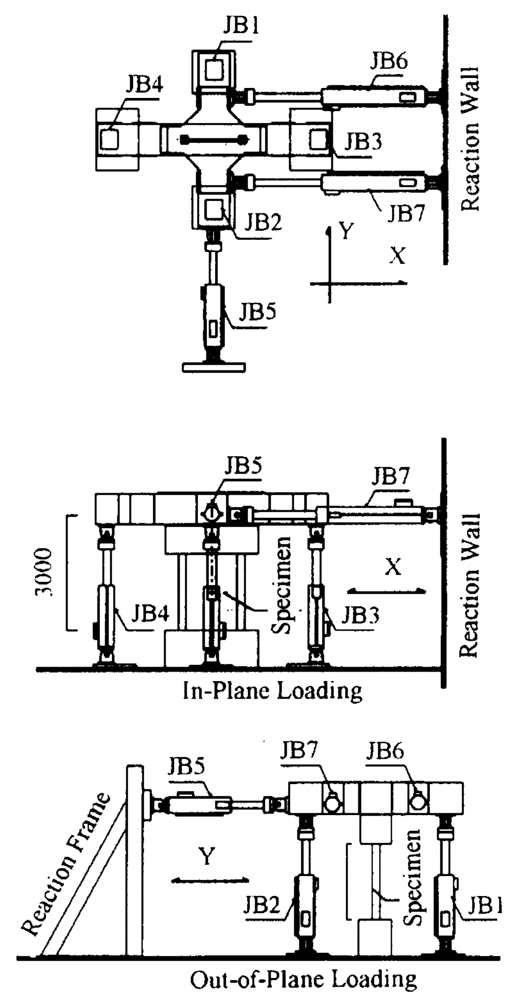

Fig. 4. The test setup of loading system

$$D_{JB1} = D_{JB2} \qquad (4)$$

where;

N_{JB1} , N_{JB2} , N_{JB3} , N_{JB4} = Axial load of actuator JB1, JB2, JB3, JB4, and

D_{JB1} , D_{JB2} = Deflection of actuator JB1, JB2.

H-shaped directional path and uni-directional path are shown in Fig. 5. The lateral loading was reversed at the deflection angle R(rad.) of 1/800, 1/400, 1/200, 1/133, 1/100, 1/67, 1/50 and 1/40. In-plane deflection was measured at the top of the wall panel. And out-of-plane deflection was measured at the middle height of wall panel. Each increment was made up of two complete reversed cycles at predetermined maximum deflection.

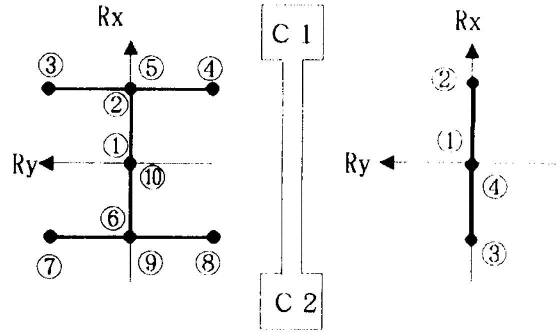

(The number indicate the order of path.)

Fig. 5. H-shaped directional path and uni-directional path

TEST RESULTS

Description of behavior

Figure 6 illustrates specimen M35X and M35H after web crushing. All specimens failed in web crushing at different displacement level. Figure 7 shows the in-plane load versus in-plane displacement relations for all specimens. Figure 8 shows the out-of-plane load versus out-of-plane displacement relations for M35H, P35H, M30H and MW35H. The load versus displacement relations was plotted directly from the recorded data. Specimen M35X under uni-directional loading failed at about Rx=1/50 in the first loading cycle. Specimen M35H under bi-directional loading failed in the second cycle of R=1/67 during out-of-plane loading. The deformation capacity of the specimens subjected to bi-lateral deformations were smaller than that of the specimen subjected to uni-lateral deformations.

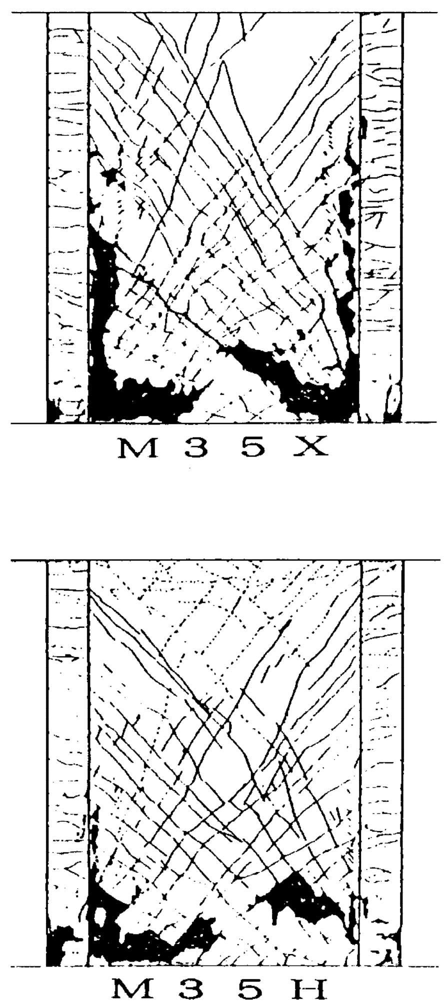

Fig. 6. Specimen M35X and M35H after web crushing

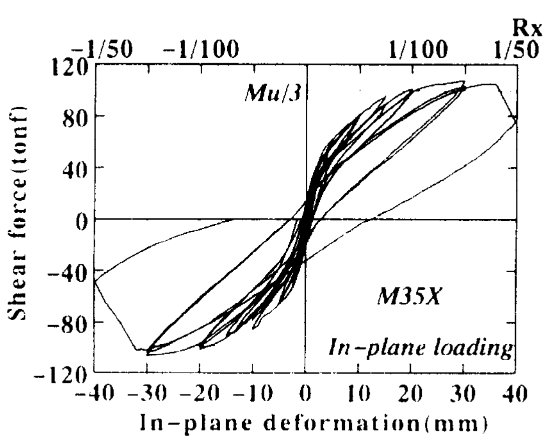

Fig. 7. Hysteressis relations (in-plane loading)

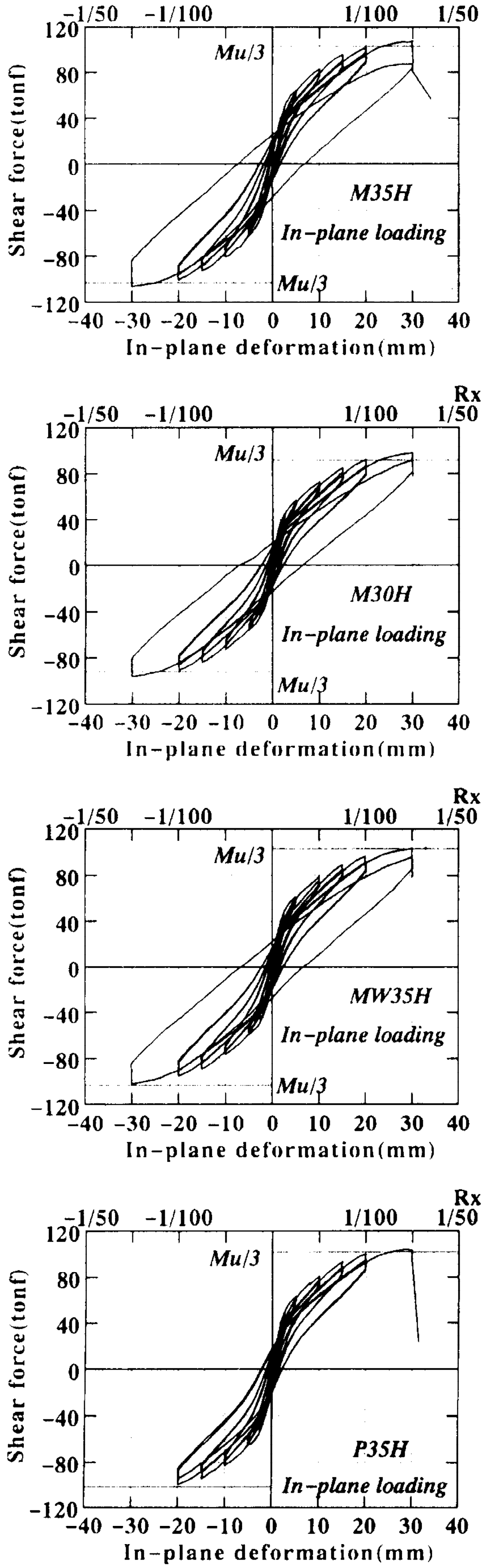

Fig. 7. Hysteressis relations (in-plane loading)

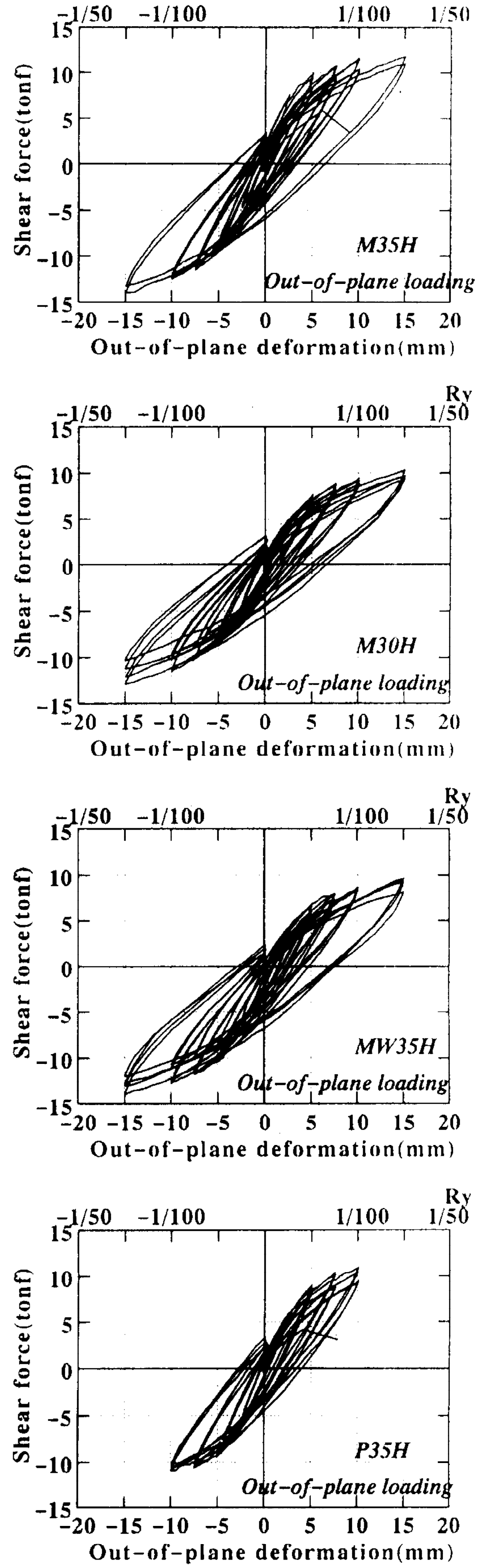

Fig. 8. Hysteressis relations (out-of-plane loading)

Specimen P35H without subties failed in the first cycle of R=1/67 during out-of-plane loading. Its deformation capacity was smaller than that of the specimen of the boundary columns with subties.
Specimen M30H under small axial load level failed in the first cycle of R=1/50 during in-plane loading. Its deformation capacity was greater than that under larger axial load level.
Specimen MW35H with additional subtie in the wall panel failed in the first cycle of R=1/50 during in-plane loading. Its deformation capacity was greater than that without none additional subtie in the wall panel.

Flexural strength

Ultimate flexural strengths of the specimens subjected to in-plane loading were calculated by the following equation (5), which is based on a flexural theory and is practically used as design equations in Japan:

$$Mu = A_t \times \sigma_y \times l_w + 0.5A_w \times \sigma_{wy} \times l_w + 0.5N \times l_w \quad (5)$$

$$Mu/3 = Mu/(l_w \times S_d) \quad (6)$$

where,

A_t, σ_y = total area and yield strength of longitudinal reinforcing bars in a column,
A_w, σ_{wy} = total area and yield strength of longitudinal reinforcing bars in wall panel,
l_w = total width of shear wall including boundary columns,
N = axial load, and
Sd = in-plane the shear span to depth ratio.

The ratios of the measured ultimate moments at the base of the specimens to the calculated as above-mentioned were 1.0 through 1.2.

Axial strains in the boundary columns and web

The relations between in-plane displacement and average axial strains in the boundary columns at the bottom within 180mm and the web near the boundary column at the bottom within 200mm shown in Fig. 9. The progress of axial strains in the boundary columns were accelerated in M35H than that of M35X because of bi-directional loading. These axial strains were less than εm in the Fig. 9 that was the ultimate strain observed in the compression test of core column element with same details (shown in Fig. 2). The axial compressive strain of M35H in the compression-side boundary column developed during out-of-plane loading as well as in-plane loading. The progress of axial strains in the web was accelerated just before the web crushing.

This strain development during out-of-plane loading as well as in-plane loading caused poor deformation capacity of shear walls subjected to bilateral deformations.

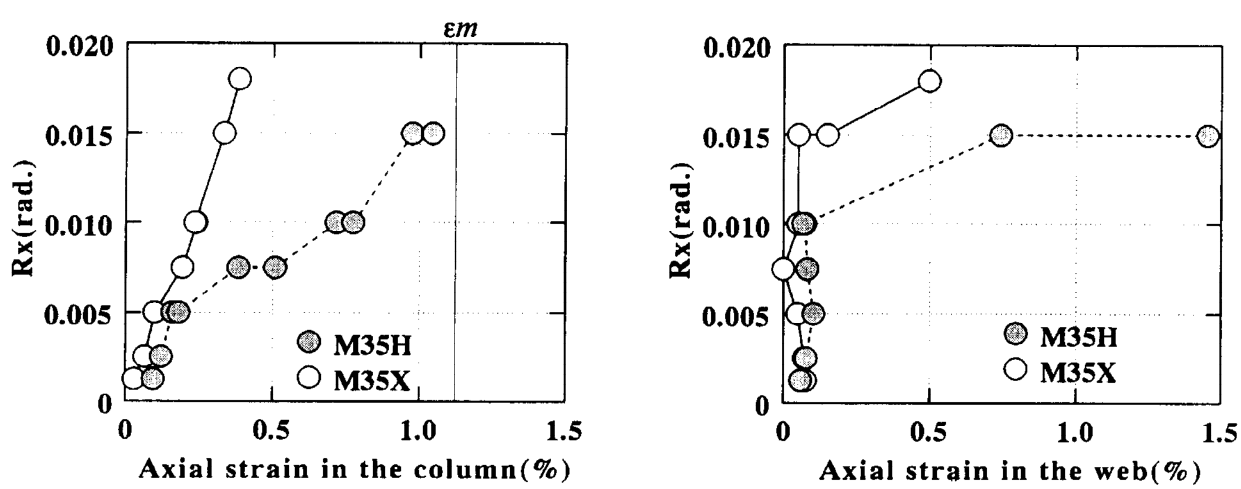

Fig. 9. Axial strains in the compression-side of the boundary columns and the web

ANALYSIS

Finite filament analysis at the base of the specimen which corresponds to the critical section was carried out for M35H based on stress-strain relations of concrete and steel to discuss the experimental results. The cross section was divided into five portions; confined concrete, concrete cover, wall panel concrete, longitudinal reinforcing in columns, and longitudinal reinforcing in wall. The analytical model for concrete is shown in Fig. 10. The uni-axial compressive strength of confined concrete obtained from the compression test of core column element with same details is used for the analysis. The bi-linear model is used for the stress-strain curves of reinforcement. Analytical loading is shown in Fig. 11.

Analytical results after in-plane deformation and after out-of-plane deformation are compared in Table 2 and Figure 12. The axial compressive strain of core concrete of compression fiber in the boundary column developed during out-of-plane loading. The axial compressive strain of the web near column developed during out-of-plane loading. The analytical results of the axial strain gave a

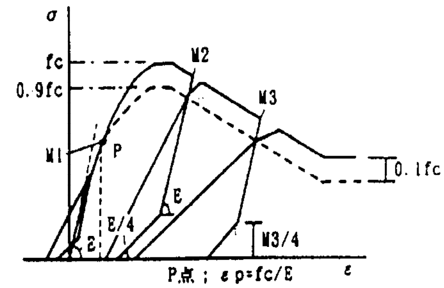

Fig.10 Concrete model (Hiraishi, et.al,1990)

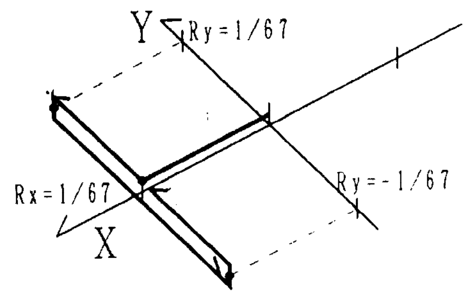

Fig.11 Analytical loading

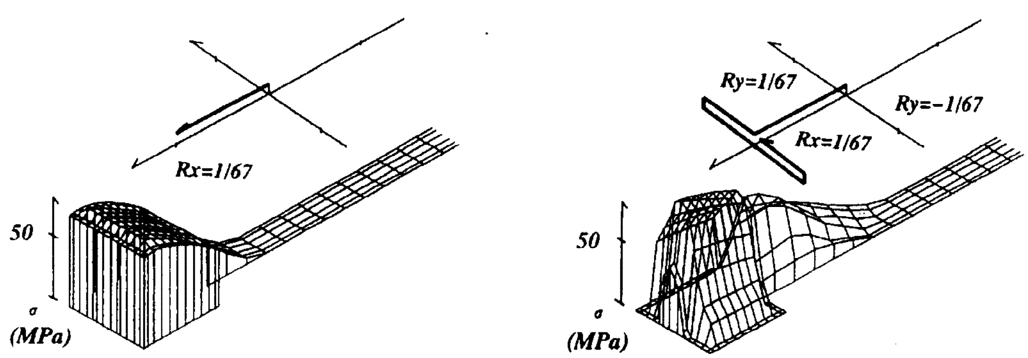

Compressive stress distribution in the critical section after in-plane deformation

Compressive stress distribution in the critical section after out-of-plane deformation

Fig. 12 Stress distributions by fiber analysis

Table 2 Analysis results

M35H Analysis	In-plane bending moment (tonf*m)	In-plane shear force (tonf)	Axial strain (%) core concrete in the column	Axial strain (%) the web near column at a distance of 25 mm	Axial force in the critical section (tonf) concrete: column	concrete: web	axial compressive force in the reinforced bar	axial tension force in the reinforced bar
Before out-of-plane loading (B)	308	103	0.33	0.11	255	23	48	-129
After out-of-plane loading (A)	219	73	0.56	0.28	162	71	39	-76
Subtract (B-A)	-89	-30	0.23	0.17	-93	48	-9	53

good agreement with the test results of M35H. During out-of-plane loading, axial force of concrete in the compression-side boundary column decreased, and axial force of concrete in the web increased. The differences of stress distributions under uni-lateral and bi-lateral loads, especially of the wall panel, are emphasized as shown in Fig. 12, which might affected the deformabilities of the shear walls.

It is concluded that when shear walls were subjected to bilateral deformations, the axial compressive strain in the compression-side boundary column developed during out-of-plane loading as well as in-plane loading, and that their deformation capacity was dominated by compression failure of the panel wall where compressive strain of concrete in-panel wall reaches to the strain which does not bearing any compression force, beyond the strain at its maximum strength. This strain development caused poor deformation capacity of shear walls subjected to bilateral deformations. However, this resisting mechanism of concrete in panel wall to axial force during out-of-plane loading delayed compression failure of boundary column of shear walls subjected to bilateral deformations under high axial load.

CONCLUSION

The following results were derived from this study:

1) All the specimens failed in web crushing.
2) The deformation capacity of the specimens subjected to bi-lateral deformations were smaller than that of the specimen subjected to uni-lateral deformation.
3) The deformation capacity of the specimen with subties in the wall or columns were larger than that without subties.
4) When shear walls were subjected to bi-lateral deformations, the axial compressive strain in the compression-side boundary column developed during out-of-plane loading as well as in-plane loading. This strain development caused poor deformation capacity of shear walls subjected to bilateral deformations.
5) The differences of stress distributions under unilateral and bilateral loading, especially that of the wall panel, are illustrated as show in Fig. 12, which might affect the deformation capacity of the walls.
6) The axial compressive strain in the compression-side boundary column developed during out-of-plane loading as well as in-plane loading. This strain development caused poor deformation capacity of shear walls subjected to bilateral deformations. The confinement of boundary column and wall panel by subtie effectively prevented the development of axial compressive strain and enhanced the deformation capacity of shear wall.

ACKNOWLEDGMENTS

This study was a part of "New RC' project promoted by Ministry of Construction of Japan. The author wishes to express his gratitude to Dr. HIRAISHI in Building Research Institute for his kindly advises. The author wishes to express his thanks to Dr. Fukuyama and Mr. Tanaka for their assistance to the test.

REFERENCE

Hiraishi, H., *et al.* (1992). Post-yield behavior of multi-story reinforced concrete shear walls subjected to bilateral deformations under axial loading. *Journal of structure and construction engineering, Architectural Institute of Japan. No. 450*, 89-97.

Hiraishi, H., *et al.* (1990). Deformation capacity beyond flexural yielding of reinforced concrete columns. *Journal of structure and construction engineering, Architectural Institute of Japan. No. 410*, 27-39.